

**KC<sub>60</sub> fulleride phase formation: An x-ray photoemission study**

D. M. Poirier and J. H. Weaver

*Department of Materials Science and Chemical Engineering, University of Minnesota, Minneapolis, Minnesota 55455*

(Received 17 February 1993)

A reversible transformation has been observed in the  $K_xC_{60}$  system, for  $0 < x < 3$ , which is characterized by a redistribution of K ions within the fcc  $C_{60}$  lattice. Below  $\sim 150^\circ\text{C}$  the tetrahedral and octahedral sites are occupied in the ratio found for  $K_3C_{60}$ , 2 to 1, and C 1s photoemission spectra indicate phase separation into  $\alpha\text{-}C_{60}$  and  $K_3C_{60}$ . Above  $\sim 150^\circ\text{C}$ , only octahedral sites are occupied for  $x < 1$ , which results in  $KC_{60}$  in the NaCl structure. Tetrahedral sites are then successively filled for  $x > 1$ , reflecting  $K_3C_{60}$  formation and coexistence with  $KC_{60}$ . These results suggest a eutectoid reaction with  $KC_{60}$  transforming into  $\alpha\text{-}C_{60}$  plus  $K_3C_{60}$ .

Incorporation of alkali metals, denoted  $A$ , into solid  $C_{60}$  has been found to proceed, in general, by the formation of discrete  $A_xC_{60}$  phases with integer values of  $x$ .<sup>1-7</sup> At room temperature, line phases with compositions  $x=3$  and 4 are now well established, as are terminal compounds of nominal composition  $x=0$  and 6 that show a small compositional range. For  $K_xC_{60}$ , synthesis can be performed at room temperature due to the facile diffusion of K into the  $C_{60}$  host.<sup>4</sup> However, incorporation is generally performed at elevated temperatures, especially for bulk samples, to speed reaction times and to improve homogeneity and crystallinity. Knowledge of the  $K_xC_{60}$  phase diagram at higher temperatures is therefore desirable. Recent Raman-scattering<sup>7</sup> and x-ray diffraction<sup>8</sup> results have identified a  $KC_{60}$  phase at elevated temperatures. With x-ray photoelectron spectroscopy (XPS), we are able to characterize  $KC_{60}$  and observe its transformation into  $\alpha\text{-}C_{60}$  plus  $K_3C_{60}$  upon cooling through  $\sim 150^\circ\text{C}$ , thereby identifying an invariant eutectoid reaction and refining the phase diagram for  $x \leq 3$ . ( $\alpha\text{-}C_{60}$  denotes the dilute solid solution of K in  $C_{60}$ .)

The XPS studies were performed using monochromatized Al  $K\alpha$  radiation ( $h\nu=1486.6$  eV, Surface Science Instruments SSX-100-03). The resolution was 0.7 eV and binding energies were referenced to the Fermi level. Chromatographically purified  $C_{60}$  powder<sup>9</sup> was evaporated from a Ta boat and condensed onto cleaved GaAs(110) in ultrahigh vacuum. A tungsten filament was used to heat the sample. The temperature was measured with an optical pyrometer that was calibrated against a Chromel-Alumel thermocouple attached to the sample face. An estimate of the uncertainty is  $\pm 10^\circ\text{C}$ . During  $C_{60}$  deposition, the sample was held at  $180^\circ\text{C}$ . Scanning-tunneling-microscopy studies<sup>10</sup> have shown epitaxial growth under these conditions with  $C_{60}(111)$  domains spanning step-free regions of the substrate and commonly attaining  $\sim 1000$  Å lateral dimensions. The  $C_{60}$  film thickness, ranging from 150 to 500 Å, was determined based on the attenuation of electrons photoemitted from the GaAs substrate.  $C_{60}$  was doped with K at  $180^\circ\text{C}$  using a SAES getter source while maintaining a chamber pressure in the low  $10^{-10}$ -Torr range. The stoichiometry was also varied by adding  $C_{60}$  to the  $K_xC_{60}$  film at  $180^\circ\text{C}$ .

Frequent contamination checks showed that the O 1s photoemission intensity was below our detection limit, indicating less than  $\sim 0.01$  at. % O.

In earlier work with  $A_xC_{60}$  we showed that the surface concentration was the same as the bulk.<sup>6</sup> Here, the samples were held at  $180^\circ\text{C}$  for  $\sim 10$  h at each stoichiometry and polar-angle-dependent XPS measurements indicated a slight deficiency of K at the surface. This high-temperature loss of K from the surface layer may indicate a thermodynamic preference for K-deficient fulleride surfaces (thermally activated surface vacancy creation). The corrected stoichiometries given herein are derived from K and C photoemission intensities (uncertainty in  $x$  of  $\pm 0.2$ ).<sup>11</sup>

Previous XPS studies of  $K_xC_{60}$  have identified K  $2p$  features associated with ions in the octahedral and tetrahedral sites of the fcc  $K_3C_{60}$  lattice.<sup>4,6,12</sup> The lower spectrum of Fig. 1 shows the K  $2p$  signature at  $25^\circ\text{C}$  acquired for a sample with  $x=0.7$ . At  $25^\circ\text{C}$ , the relevant portion of the  $K_xC_{60}$  phase diagram indicates that the sample is composed of regions of  $K_3C_{60}$  and  $\alpha\text{-}C_{60}$ .<sup>1,3-6</sup> Since the solubility of K in  $\alpha\text{-}C_{60}$  is small ( $x_{\text{max}} \sim 0.1$ , Ref. 6), this spectrum represents the K  $2p$  signature of  $K_3C_{60}$ . Stoichiometry-dependent results show that the K  $2p$  line shape at  $25^\circ\text{C}$  is nearly unchanged for  $x$  between 0 and 3 with account taken of the background from the C 1s satellites. The K  $2p$  doublets labeled  $T$  and  $O$  are due to ions in tetrahedral and octahedral sites, respectively. The binding energy difference, 1.17 eV, is determined largely by a difference in the local Madelung potentials. In  $K_3C_{60}$ , all tetrahedral and octahedral sites are occupied and the intensity ratio of the corresponding features is 2:1.

The top spectrum of Fig. 1, obtained from the same sample at  $180^\circ\text{C}$ , shows a single doublet corresponding to K in octahedral sites. The depopulation of tetrahedral sites begins as the temperature is increased above  $\sim 150^\circ\text{C}$ . This change in site occupancy is completely reversible over multiple heating and cooling cycles and is also reflected in the K  $3s$  and K  $3p$  core-level spectra. X-ray diffraction results<sup>8</sup> show a transformation to a  $KC_{60}$  phase (NaCl structure) that is completed by  $\sim 180^\circ\text{C}$ , in agreement with the exclusive occupancy of octahedral

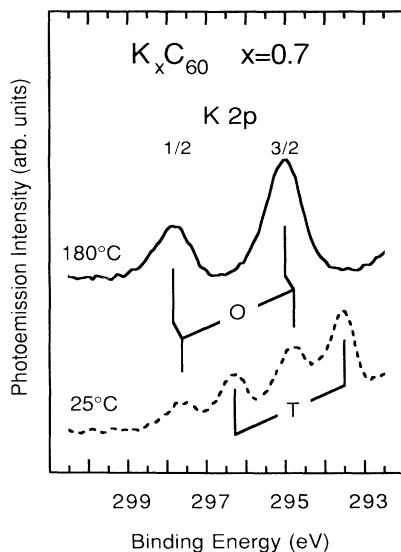


FIG. 1. K  $2p$  photoemission spectra ( $h\nu=1486.6$  eV) for  $K_{0.7}C_{60}$ . The sample is a mixture of  $\alpha$ - $C_{60}$  and  $K_3C_{60}$  at  $25^\circ\text{C}$  characterized by tetrahedrally and octahedrally coordinated  $K^+$  ions in a 2:1 ratio, as identified for the inequivalent features labeled  $T$  and  $O$ . For  $T > 150^\circ\text{C}$ , K ions vacate the tetrahedral sites, occupying only the larger octahedral sites and forming  $KC_{60}$  with the NaCl structure.

sites. Raman-scattering experiments<sup>7</sup> have also indicated a phase characterized by unity negative charge on the  $C_{60}$  molecules, although at a somewhat lower temperature.

Figure 2 shows how the K  $2p$  spectra evolve with increasing K content at  $180^\circ\text{C}$  (solid lines) and  $25^\circ\text{C}$  (dashed lines). The spectra are normalized to give approximately constant K  $2p$  intensities. The room-temperature results show a  $K_3C_{60}$  signature that grows on the sloping background of the C  $1s$  satellite structure for  $x < 3$ , as demonstrated by Poirier *et al.*,<sup>6</sup> with minimal change in K  $2p$  line shape. Only when there is a significant fraction of  $\alpha$ - $C_{60}$  is this trend violated, e.g.,  $x=0.4$ , but this is expected since the dilute phase is characterized by preferential octahedral site occupancy.<sup>6</sup> Analysis of the spectra for  $x > 3$  shows that a new K  $2p$  doublet emerges between the  $O$  and  $T$  features as  $K_4C_{60}$  is produced.

The spectra in Fig. 2 show a very different evolution at  $180^\circ\text{C}$  (solid lines) since they demonstrate only octahedral site occupation until  $x \sim 1$ . Beyond  $x \sim 1$ , the tetrahedral holes begin to fill. The tetrahedral contribution grows and, finally, the  $K_3C_{60}$  signature is obtained. At the final  $K_3C_{60}$  state, the spectra are unchanged from  $25^\circ\text{C}$  to  $180^\circ\text{C}$ . Hence, interstitial sites are occupied in the ratio found for  $K_3C_{60}$  at  $25^\circ\text{C}$  for  $x \leq 3$  while K ions avoid tetrahedral sites at  $180^\circ\text{C}$  until the octahedral sites have been completely filled.

Examination of the C  $1s$  spectra at  $25^\circ\text{C}$  shows that the signatures of both  $\alpha$ - $C_{60}$  and  $K_3C_{60}$  are present for any value of  $x$  less than 3, reflecting the two-phase character of the sample.<sup>6</sup> Figure 3 shows the spectrum for  $K_{1.2}C_{60}$ . The narrow peak at 285.1 eV represents  $\alpha$ - $C_{60}$ . The  $K_3C_{60}$  signature first emerges as a low binding energy

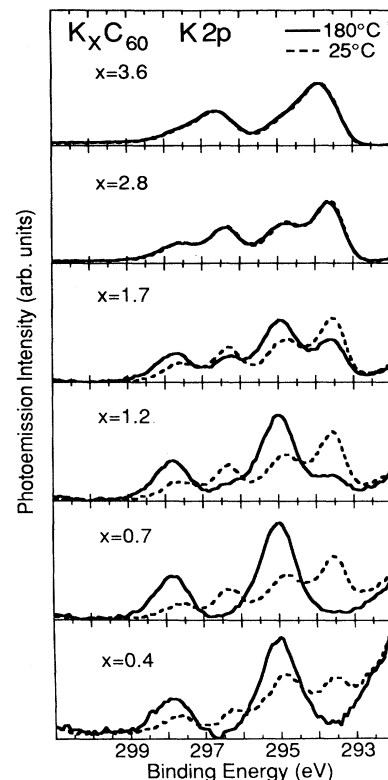


FIG. 2. K  $2p$  spectra, as in Fig. 1, for representative stoichiometries. The solid lines show only octahedral site occupancy for  $x < 1$  at  $180^\circ\text{C}$ . The dashed spectra show the  $K_3C_{60}$  signature for  $x < 3$  at  $25^\circ\text{C}$ . The rising background at low binding energy is due to overlapping C  $1s$  satellite structure. The spectra are dominated by the  $K_3C_{60}$  signature at  $x=2.8$ , independent of temperature, and the signature of  $K_4C_{60}$  emerges beyond  $x=3$ .

shoulder for  $x=0.4$  but eventually dominates the C  $1s$  emission for  $x=2.8$ . Spectra at intermediate compositions, as in Fig. 3, represent superpositions of these signatures. A partial decomposition is shown in Fig. 3 where the C  $1s$  feature obtained for  $x=2.8$  has been scaled appropriately and is shown by unconnected data points. The center of mass of the C  $1s$  feature moves to lower binding energy as K is added, consistent with an increase in average negative charge on the  $C_{60}$  molecules.  $KC_{60}$  continues this trend since the spectra obtained upon heating to  $180^\circ\text{C}$  show a shift in spectral weight to an energy intermediate to those found for  $\alpha$ - $C_{60}$  ( $x \cong 0$ ) and  $K_3C_{60}$ . Thermal broadening was found to be negligible between  $25^\circ\text{C}$  and  $\sim 140^\circ\text{C}$  and could not account for the large temperature-dependent changes in line shape. As for the K  $2p$  results, there is little temperature dependence for  $x > 3$ .

The original fulleride phase diagram proposed by Zhu *et al.*<sup>1</sup> suggested a miscibility gap between  $\alpha$ - $C_{60}$  and  $A_3C_{60}$  based on results for  $Rb_xC_{60}$ . In this scheme the solubility limits of  $A$  in  $\alpha$ - $C_{60}$  and of  $A$  vacancies in  $A_3C_{60}$  would increase with temperature until the phase boundaries met, producing a single-phase region for  $0 < x < 3$ . Subsequent work<sup>3,6,13</sup> showed that a generic

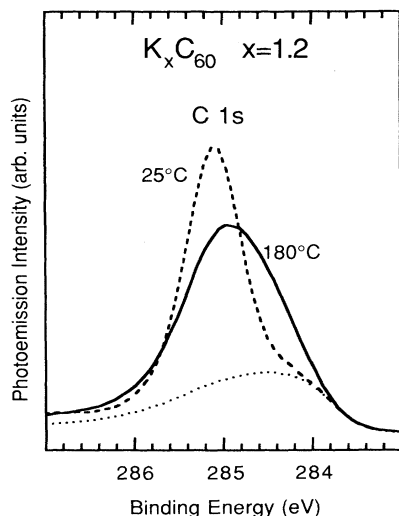


FIG. 3. C 1s spectra for  $K_{1.2}C_{60}$ . At 25°C, the  $\alpha-C_{60}$  signature (peak at 285.1 eV) and the  $K_3C_{60}$  signature are present. The unconnected data points show the C 1s spectrum for  $x=2.8$  appropriately scaled to show the  $K_3C_{60}$  contribution at 25°C. At 180°C, the C 1s peak is dominated by a  $KC_{60}$  contribution and is centered between the  $\alpha-C_{60}$  and  $K_3C_{60}$  features.

phase diagram does not exist for the alkali-metal fullerenes. From the XPS results for  $K_xC_{60}$ , we propose an alternate phase diagram which includes an invariant eutectoid reaction  $KC_{60} \rightleftharpoons \alpha-C_{60} + K_3C_{60}$ .

The eutectoid phase diagram of Fig. 4 identifies the transformation of  $KC_{60}$  into  $\alpha-C_{60}$  plus  $K_3C_{60}$  upon cooling below  $\sim 150^\circ\text{C}$ . This transition temperature is independent of stoichiometry between the phase boundaries and the relative amounts of the constituents follow the lever rule. Figure 4 shows that the transition temperatures measured upon heating are constant within experimental uncertainty.<sup>14</sup> The observed reactions were completed over a  $\sim 20^\circ\text{C}$  range of temperature on a time scale of  $\sim 30$  min. There was hysteresis over a cooling and warming cycle, as expected since the reaction temperature defines the start of the forward and reverse transformations and some degree of undercooling may be necessary for the forward (cooling) transformation to proceed at an observable rate.

The eutectoid phase diagram stipulates coexistence of  $\alpha-C_{60}$  and  $KC_{60}$  above  $\sim 150^\circ\text{C}$  for  $\sim 0.2 < x < 1$ . The binding energy of the K 2p octahedral feature is invariant with  $x$  and this supports the phase separation picture. This insensitivity to  $x$  suggests a well-defined octahedral site Madelung potential of the sort found for phase-separated regions of  $KC_{60}$  but not for K ions randomly distributed in a solid solution. While the XPS results clearly show the absence of tetrahedral site occupation in this region for either  $\alpha-C_{60}$  or  $KC_{60}$ , the broad C 1s features are less informative.

The eutectoid phase diagram shows coexistence of  $K_3C_{60}$  and  $KC_{60}$  between  $x=1$  and 3 for  $T > 150^\circ\text{C}$ . In this region, the binding energy of the tetrahedral component appears in the position expected for  $K_3C_{60}$  and does not change with stoichiometry. Line-shape analysis shows the evolution that would be expected if the octahe-

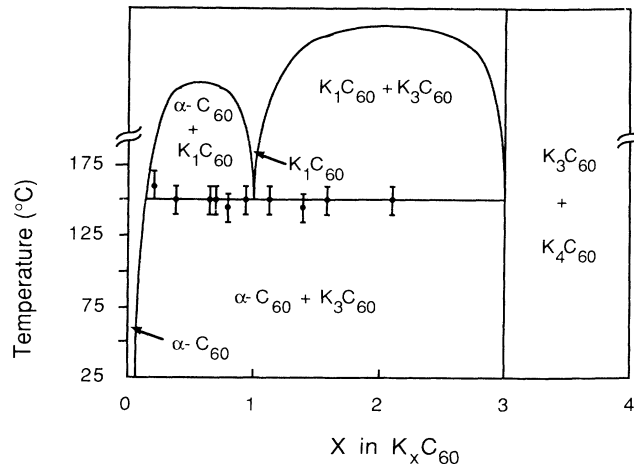


FIG. 4. Proposed binary phase diagram for  $K_xC_{60}$  showing a eutectoid transformation  $KC_{60} \rightleftharpoons \alpha-C_{60} + K_3C_{60}$  at  $150^\circ\text{C}$ . The measured transition temperatures are indicated by data points. The upper limit of our experimental data is indicated by a break in the temperature axis beyond which no firm temperature scale is implied. We speculate that the two phase regions above the eutectoid are defined by miscibility gaps.

dral feature of  $K_3C_{60}$  replaced that of  $KC_{60}$  with increasing  $x$ . For the C 1s feature, decomposition into  $KC_{60}$  and  $K_3C_{60}$  components can be done, though less convincingly than for the sharply contrasting  $\alpha-C_{60}$  and  $K_3C_{60}$  signatures at room temperature.<sup>6</sup> We note that the Raman-scattering results support this picture of a two-phase region for  $1 < x < 3$  although the apparent transition temperature is lower.<sup>7</sup> We speculate that the two-phase regions above  $\sim 150^\circ\text{C}$  may represent dual miscibility gaps, as drawn, but a firm temperature scale must await measurements at higher temperature than could be achieved with thin films *in vacuo*.

The redistribution of K ions associated with the eutectoid transformation reflects a destabilization of  $K_3C_{60}$  relative to  $KC_{60}$ . This is probably the result of increased  $C_{60}$  motion and the consequent change in size of the tetrahedral holes of the lattice. The radii of  $C_{60}$  and  $K^+$  suggest a tight fit for K in the tetrahedral sites, leading Stephens *et al.*<sup>15</sup> to suggest that the  $C_{60}$  molecules are locked in place with hexagons facing tetrahedral sites in order to accommodate the cations. Nuclear magnetic resonance (NMR) studies indicate that the speed of  $C_{60}$  rotational diffusion is decreased in  $K_3C_{60}$  with respect to the pure fullerene solid<sup>5</sup> and this is presumably the result of steric interaction with the K ions. With increased temperature, the  $C_{60}$  molecules reorient more rapidly<sup>16</sup> and the hexagonal "dimples" will not face the tetrahedral K ions simultaneously. This effect, coupled with increased intermolecular vibrational amplitudes, reduces the effective size of the tetrahedral site and forces a compensating expansion of the lattice. This reduces the stabilizing Madelung energy and the free energy of  $K_3C_{60}$  increases relative to  $KC_{60}$ . The transformation is accomplished as tetrahedrally coordinated K ions migrate to vacant octahedral sites of neighboring  $\alpha-C_{60}$  domains,

converting the  $\alpha$  phase to  $\text{KC}_{60}$  around the nucleus of the old  $\text{K}_3\text{C}_{60}$  grain. This would proceed until all vacant octahedral sites were occupied or until all the  $\text{K}_3\text{C}_{60}$  had "dissolved," depending on the global stoichiometry. While the  $\text{KC}_{60}$  phase should be less favorable in terms of the Madelung energy,<sup>3</sup> it is probably preferred on steric grounds. X-ray diffraction results indicate that the lattice constant of  $\text{KC}_{60}$  is smaller than that of  $\text{K}_3\text{C}_{60}$  and, in fact, smaller than that of pure  $\text{C}_{60}$ , thereby supporting the hypothesis that the  $\text{K}_3\text{C}_{60}$  lattice is sterically limited.

In addition to  $\text{KC}_{60}$  in the NaCl structure, x-ray diffraction experiments<sup>8</sup> suggest a disordered fcc "lattice gas" at  $x = 1$ , with K ions occupying tetrahedral and octahedral sites between  $\sim 150^\circ\text{C}$  and  $\sim 70^\circ\text{C}$  in a 2:1 ratio. Below  $\sim 70^\circ\text{C}$  they suggest a third  $\text{KC}_{60}$  structure, with rhombohedral symmetry, that persists to zero degrees Kelvin. Evidence of a second transition of some type is corroborated by differential scanning calorimetry.<sup>8</sup> Careful inspection of the XPS spectra yields no evidence for these additional structures. We find that the high-resolution C 1s spectra are identical between  $25^\circ\text{C}$  and  $\sim 140^\circ\text{C}$  and are derived from two features, thereby indicating at least two inequivalent chemical environments for C. Significantly, the two C 1s signatures are those found for  $x \sim 0$  and 3 and the spectra can be decomposed into appropriate amounts of the  $\text{K}_3\text{C}_{60}$  and  $\alpha\text{-C}_{60}$  signatures for  $0 \leq x \leq 3$  (Ref. 6).

The mixed-site occupation of  $\text{KC}_{60}$  is in stark contrast to results for  $\text{RbC}_{60}$  and  $\text{CsC}_{60}$  where the spectroscopic results showed exclusively octahedral site occupancy and a single C 1s feature at  $25^\circ\text{C}$ .<sup>6</sup> NMR results<sup>17</sup> also indicate a similar distinction between  $\text{KC}_{60}$  and the  $\text{AC}_{60}$  phases of the heavier alkali metals. XPS investigations of  $\text{RbC}_{60}$  showed no spectral change between  $25^\circ\text{C}$  and  $175^\circ\text{C}$ , bridging the regime around  $60^\circ\text{C}$  where x-ray diffraction results indicate that the high-temperature

NaCl structure distorts to rhombohedral symmetry.<sup>8</sup> While XPS is not expected to be sensitive to a slight change in symmetry, there remains a fundamental discrepancy in the case of  $\text{K}_x\text{C}_{60}$  because the x-ray diffraction results indicate a single phase at room temperature while the XPS, Raman,<sup>7</sup> and NMR (Ref. 5) results indicate a two-phase region for  $0 < x < 3$ .

The presence of a eutectoid transformation has important implications for synthesis of  $\text{K}_x\text{C}_{60}$  samples with  $x < 3$ . Specifically, if the sample is heated above  $\sim 150^\circ\text{C}$ , it will transform partially to  $\text{KC}_{60}$  and rapid cooling will quench in this high-temperature structure. In our case, we were able to quench in a large portion of  $\text{KC}_{60}$  by cooling with a thermal time constant of  $\sim 10$  min. In contrast, holding the sample just below the eutectoid temperature for long periods of time should result in large grains in the mixed-phase samples. Variations in the cooling schedule may produce a variety of microstructures.<sup>18</sup>

In summary, we have observed a reversible transformation from  $\text{KC}_{60}$  into  $\alpha\text{-C}_{60}$  plus  $\text{K}_3\text{C}_{60}$ . The eutectoid temperature is  $(150 \pm 10)^\circ\text{C}$ . Coexistence of  $\text{KC}_{60}$  and  $\text{K}_3\text{C}_{60}$  is found above  $\sim 150^\circ\text{C}$  for  $1 < x < 3$ . For  $0 < x < 1$ , we show evidence for a mixture of  $\text{KC}_{60}$  and  $\alpha\text{-C}_{60}$  above  $\sim 150^\circ\text{C}$  although the possibility of an interstitial solid solution in which K ions randomly occupy the octahedral sites of the  $\text{C}_{60}$  host lattice cannot be completely ruled out. At room temperature,  $\text{K}_x\text{C}_{60}$  consists of phase separated  $\alpha\text{-C}_{60}$  and  $\text{K}_3\text{C}_{60}$  for  $0 < x < 3$ .

This work was supported by the National Science Foundation and the Office of Naval Research. Purified  $\text{C}_{60}$  was generously provided by R. E. Smalley and L. P. F. Chibante. We thank F. Stepniak and P. J. Benning for helpful discussions and H. Kuzmany, J. E. Fischer, and R. Tycko for sharing results prior to publication.

- <sup>1</sup>Q. Zhu *et al.*, *Science* **254**, 545 (1991); O. Zhou and D. E. Cox, *J. Phys. Chem. Solids* **53**, 1373 (1992).
- <sup>2</sup>P. W. Stephens *et al.*, *Phys. Rev. B* **45**, 543 (1992).
- <sup>3</sup>R. M. Fleming *et al.*, *Nature* **352**, 701 (1991); D. W. Murphy *et al.*, *J. Phys. Chem. Solids* **53**, 1321 (1992).
- <sup>4</sup>D. M. Poirier, T. R. Ohno, G. H. Kroll, Y. Chen, P. J. Benning, J. H. Weaver, L. P. F. Chibante, and R. E. Smalley, *Science* **253**, 646 (1991).
- <sup>5</sup>R. Tycko, G. Dabbagh, M. J. Rosseinsky, D. W. Murphy, R. M. Fleming, A. P. Ramirez, and J. C. Tully, *Science* **253**, 884 (1991).
- <sup>6</sup>D. M. Poirier, T. R. Ohno, G. H. Kroll, P. J. Benning, F. Stepniak, J. H. Weaver, L. P. F. Chibante, and R. E. Smalley, *Phys. Rev. B* (to be published).
- <sup>7</sup>J. Winter and H. Kuzmany, *Solid State Commun.* **84**, 935 (1992).
- <sup>8</sup>J. E. Fischer and Q. Zhu (private communication).
- <sup>9</sup>R. E. Haufler *et al.*, in *Clusters and Cluster-Assembled Materials*, edited by R. S. Averback, J. Bernholc, and D. L. Nelson, MRS Symposia Proceedings No. 206 (Materials Research Society, Pittsburgh, 1991), p. 627; *J. Phys. Chem.* **94**, 8634 (1990).
- <sup>10</sup>Y. Z. Li, J. C. Patrin, M. Chander, J. H. Weaver, L. P. F. Chibante, and R. E. Smalley, *Phys. Rev. B* **46**, 12 914 (1992); Y. B. Zhao, D. M. Poirier, and J. H. Weaver (unpublished).
- <sup>11</sup>The surface K deficiency was modeled as a  $\text{K}_0\text{C}_{60}$  overlayer on an ideal fulleride surface. The thickness of the overlayer was calculated based on the variation in measured K content with the change in probe depth affected by varying the detection angle (assuming an electron mean free path of  $25 \text{ \AA}$ ). The stoichiometry was adjusted to account for attenuation of the K signal by this virtual overlayer. Calculated overlayer thicknesses were a fraction of a  $\text{C}_{60}$  diameter.
- <sup>12</sup>P. J. Benning, D. M. Poirier, T. R. Ohno, Y. Chen, F. Stepniak, G. H. Kroll, J. H. Weaver, J. Fure, and R. E. Smalley, *Phys. Rev. B* **45**, 6899 (1992).
- <sup>13</sup>M. J. Rosseinsky, D. W. Murphy, R. M. Fleming, R. Tycko, A. P. Ramirez, T. Siegrist, G. Dabbagh, and S. E. Barrett, *Nature* **356**, 416 (1992).
- <sup>14</sup>The transition temperature was defined as the temperature at which the octahedral and tetrahedral site occupancy was first significantly altered as the sample was heated.
- <sup>15</sup>P. W. Stephens, L. Mihaly, P. L. Lee, R. L. Whetten, S.-M. Huang, R. Kaner, F. Diederich, and K. Holczer, *Nature* **351**, 632 (1991).
- <sup>16</sup>S. E. Barrett and R. Tycko, *Phys. Rev. Lett.* **69**, 3754 (1993).
- <sup>17</sup>R. Tycko (private communication).
- <sup>18</sup>W. D. Callister, Jr., *Materials Science and Engineering: An Introduction* (Wiley, New York, 1985), Chap. 9.